

Analysis of Environmentally Friendly Refrigerant Options for Window Air Conditioners

ABSTRACT

This paper presents a technical assessment of environmentally friendly refrigerants as alternatives to R410A for window air conditioners. The alternative refrigerants that are studied for its replacement include R32, a mixture of R32/R125 with 90%/10% molar concentration, R600a, R290, R1234yf, R1234ze and R134a. Baseline experiments were performed on a window unit charged with R410A. The heat pump design model (HPDM) was modified and calibrated with the baseline data and was used to evaluate the comparative performance of the window air conditioner (WAC) with alternative refrigerants. The paper discusses the advantages and disadvantages of each refrigerant and their suitability for window air conditioners. Among all the refrigerants studied, R32 offers the best efficiency improvement over R410A and has a 67.5% lower Global Warming Potential (GWP).

Key Words: EER, Window air conditioner, alternative refrigerants, model, slinger

1. INTRODUCTION

Window air conditioners (WAC) are cheap and sold in large numbers internationally as a low-cost means to provide cooling and improve comfort in older buildings that lack ducted systems, and in cases where a central system upgrade is too expensive [Shen and Bansal (2014), Nogueira (2013), Winker et al. (2013)]. According to the US Energy Information Administration (EIA) there were nearly 46.7 million WACs operating within the United States in 2009 [EIA (2009)], accounting for approximately 1.5% of the total US residential energy use or about 0.33 quads (0.35 EJ). Due to global warming and other environmental concerns, there is a pressing need to find an alternative to the currently used refrigerant R410A with smaller Global Warming Potential (GWP) in order to reduce the greenhouse gas emissions and protect the environment. There are several alternative refrigerant options available, including R32, R600a, R290, R1234yf and R1234ze; however, all of these are either flammable or slightly flammable.

This manuscript has been authored by UT-Battelle, LLC under Contract No. DE-AC05-00OR22725 with the U.S. Department of Energy. The United States Government retains and the publisher, by accepting the article for publication, acknowledges that the United States Government retains a non-exclusive, paid-up, irrevocable, world-wide license to publish or reproduce the published form of this manuscript, or allow others to do so, for United States Government purposes. The Department of Energy will provide public access to these results of federally sponsored research in accordance with the DOE Public Access Plan (<http://energy.gov/downloads/doe-public-access-plan>)

Due to the compact size configuration and small refrigerant charge of R410A in a WAC (less than 1 kg), the flammability of the refrigerant is less of a concern. Because of this, these refrigerants can be evaluated as potential alternatives to R410A. This study documents the details of a WAC unit charged with R410A, and its testing in the laboratory environment, specifically the effectiveness of the sub-merged sub-cooler and the slinger in the performance improvement of the WAC. Based on the test data, a heat pump design model (HPDM) [Shen and Rice (2014), Rice et al. (1981)] was modified to include specific features of a WAC (e.g., the sling effect and the sub-merged sub-cooler). The model has the unique capability of analyzing a heat exchanger using the segment-by-segment approach. This model was calibrated against the baseline experimental data and then used to perform parametric analyses to assess the performance of the WAC with alternative refrigerants including R32, mixture of R32/R125 with 90/10 molar concentration, R600a, R290, R1234yf, R1234ze and R134a. The paper discusses the relative merits of each refrigerant on the system performance.

2. SYSTEM CONFIGURATION AND DESIGN DETAILS

A WAC having a nominal cooling capacity of 10,000 Btu/hr (2.93 kW) was extensively tested in an environmental chamber and modeled. The WAC has a single-speed rotary compressor, a fin-&-tube evaporator and condenser, a capillary tube expansion device and a motor mounted on a single axis shaft to drive both the evaporator blower and the condenser fan. In addition to these basic components, the WAC has a fin-&-tube sub-cooler, submerged in the condensate water collection pan. The submerged sub-cooler is downstream of the air-to-refrigerant condenser to further subcool the liquid refrigerant. The schematic diagram of the WAC and its P-h diagram are shown in Figures 1 and 2 respectively. The condenser fan blade is specially configured, to pick up water from the water collection pan and to spray it in the air stream flowing over the condenser coil surface. The water droplets evaporate and enhance the condenser heat transfer. This feature is called the “sling” effect. Figures 3, 4 and 5 respectively show the single axis fan, the “slinger ring” and instrumented WAC. Some of the basic parameters of the evaporator and condenser are given in Table 1. This unit was fully instrumented including a Coriolis refrigerant mass flow sensor, 3 in-line refrigerant temperature transducers (at suction, discharge and liquid line), 4 refrigerant side pressure transducers, 11 refrigerant tube wall temperature thermocouples, 24 air-side temperature thermocouples, 4 air side relative humidity measurements, 3 power

measurements including fan, compressor, and total power; and a barometric pressure. The sensor uncertainties are given in Table 2.

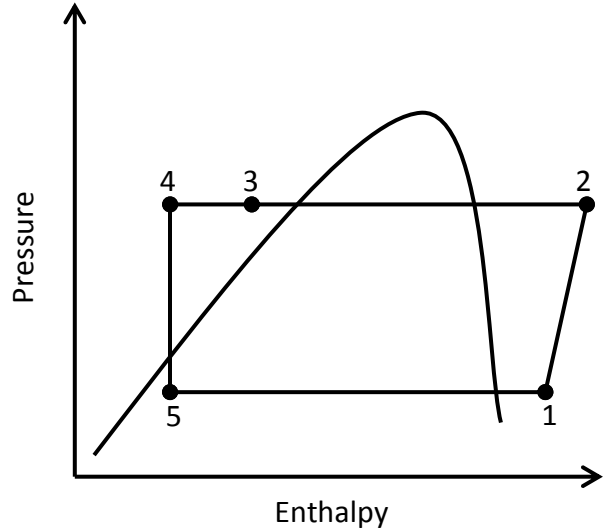
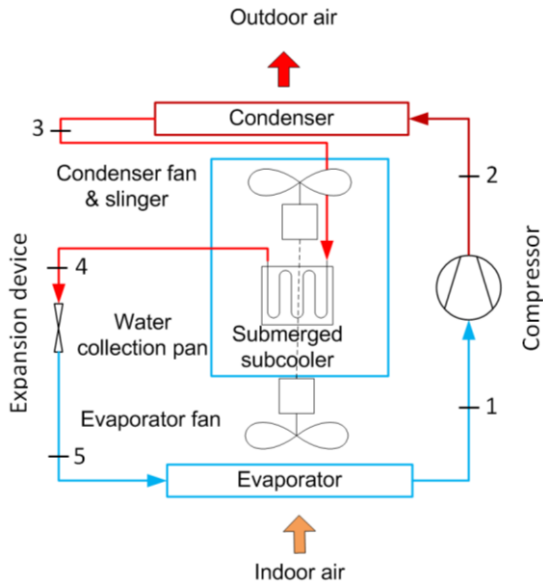


Figure 1: Schematics of Window Air Conditioner **Figure 2:** P-h diagram of Window Air Conditioner



Figure 3: Single axis blower/fan

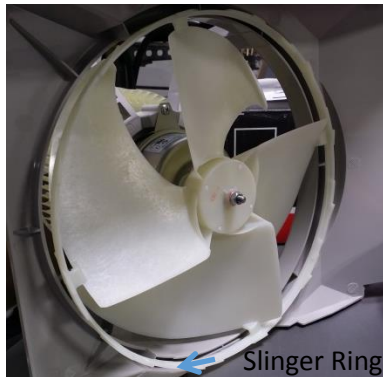


Figure 4: Slinger on condenser fan



Figure 5: Instrumented WAC

Table 1: Condenser and Evaporator of Window Air Conditioner

Parameters	Fin-&-Tube Condenser Coil	Fin-&-Tube Evaporator Coil
Face area [ft ² (m ²)]	1.356 (0.171)	0.797 (0.100)
Total Tube Number	48	48
Number of rows	3 (cross counter-flow)	4 (cross counter-flow)
Number of parallel circuits	4	3

At the standard single point rating conditions of WAC [DOE (2011), e-CFR(2014)], i.e. outdoor dry bulb/wet bulb temperatures of 95°F/75°F (35°C/23.9°C) and indoor dry bulb/wet bulb temperatures of 80°F/67°F (26.7°C/19.4°C), the corresponding compressor isentropic and volumetric efficiencies are taken as 66% and 86% respectively, from the manufacturer’s manual. The compressor shell heat loss ratio, relative to the compressor power, is assumed to be 20%. In this study, the WAC was extensively tested over a range of operation conditions. The experimental data was used to calibrate the HPDM for the WAC to match the measured performance. Simulations were performed for multiple alternative refrigerants, e.g. R32, R600a, R290, R1234yf, R1234ze, and a mixture of R32/R125 with molar concentrations of 90%/10%. The GWPs of these refrigerants are given in Table 3. For example, the use of R32 or the blended mixture of R32 (90% molar concentration)/R125 (10% molar concentration) have GWPs that are about 67.5% and 40% lower than that of R410A, respectively. These features were assessed in view of the environmental friendliness of future WACs.

All refrigerant properties were calculated using REFPROP 9.1 [Lemmon et al. (2013)]. The comparisons are presented in terms of efficiency, compressor displacement volume, heat exchanger saturation temperature changes, and compressor discharge temperature.

Table 2: Sensors uncertainty analysis

Measurement	Estimated Sensor Uncertainty
Temperature	±.25 F
Refrigerant Pressure (low)	±.2 psi
Refrigerant Pressure (high)	±.6 psi
Mass Flow Rate	±.7 lbm/hr
Electrical Power (fan)	±2 W
Electrical Power (compressor and system total)	±10 W
Atmospheric Pressure	±.009 psi
Relative Humidity	±1.4 %RH

Table 3: Global Warming Potential (GWP) of the Alternative Refrigerants

	R410A	R32	R134a	R600a	R290	R1234yf	R1234ze	R32-90%/R125-10%
GWP	2079	675	1430	20	20	4	6	1251

3. HPDM WITH SPECIFIC FEATURES OF WINDOW AIR CONDITIONER AND ITS VALIDATION

The HPDM is a hardware-based steady-state component-based simulation model that uses the Newton-Raphson method to solve simultaneous system equations. The component HX models have different levels of complexity, which fall into three categories, i.e. bulk models, phase-to-phase models, and discretized models. These are used to build a heat exchanger having arbitrary circuitry, geometry, and represent any boundary conditions. All phase-to-phase and segment-to-segment heat exchanger models are capable of calculating refrigerant charge inventory. For the system modeling, a component-based modeling framework has been developed that allows connecting steady-state component models in any manner. It may be noted here that the main objective of the experimental and modeling work is to compare the EERs of WAC with various alternative refrigerants at a single operation condition, i.e. indoor 80°F DB/67°F WB (26.7°C/19.4°C) and 95°F DB/75°F WB (35°C/23.9°C) outdoor air temperature. Details of some of the component models are described below.

Compressor: HPDM provides multiple choices per AHRI standard 540 [ANSI/AHRI (2007)] for modeling a single-speed compressor; however, a 10-coefficient compressor map has been used here to model the baseline WAC unit using R410A. It simulates energy balance from inlet to outlet using the calculated power and given heat loss ratio; and it also considers the actual suction state to correct the map mass flow predictions. Since the compressor maps are not available for other alternative refrigerants being considered in this study, constant values of volumetric efficiency, isentropic efficiency, compressor displacement volume and rotational speed (3500 RPM) have been used.

Heat Exchangers: A segment-to-segment modeling approach has been used here where each tube segment has individual air side and refrigerant side entering states, and may have possible phase transition. Within each segment, an ε -NTU approach is used for heat transfer calculations and the air-side fin is simplified as an equivalent annular fin. Both refrigerant and air-side heat transfer and pressure drops are considered. The coil model can simulate arbitrary tube and fin geometries and circuitries and any entering and exit states of refrigerant, misdistribution, two-dimensional air side temperature, and local inputs of humidity and velocity. The tube circuitry and 2-D boundary conditions are provided by an input file. The segment-to-segment modeling

approach is also capable of simulating the dehumidification process of water condensing on an HX coil (i.e. evaporator) by following Braun et al. (1989) methodology, where the driving potential for heat and mass transfer is the enthalpy difference between the inlet air and the saturated air at the refrigerant temperature.

It should be noted that the flow-pattern-dependent heat transfer correlations published by Thome and El Hajal (2002) and Thome et al (2003a, 2003b) are adopted to calculate the tube side evaporation and condensation heat transfer coefficients. The most reasonable approaches for modeling two-phase heat transfer and pressure drop involve two-phase flow pattern analysis. The flow-pattern-dependent models obtain two-phase heat transfer coefficients specific to the local flow pattern distribution; the heat transfer model is coupled with the flow map.

Expansion Device: Expansion device was modeled as an isenthalpic process where both the degrees of superheat and sub-cooling were specified as inputs.

Fans and Blowers: For a given airflow rate, the model normally uses the fan curve to simulate static head, power consumption, and calculate air-side temperature increment from inlet to outlet. However, in this study, we did not use a fan curve. Instead, we directly used the air flow rate and the corresponding power consumption measured in the experiment.

Submerged sub-cooler: The sub-cooler model considers phase transition in the heat transfer section, i.e. allowing two-phase or liquid refrigerant entrance [LBNL (1997)]. It assumes natural convection at the water side. The water pool temperature is a measured input. Effectiveness-NTU method is used to calculate energy transfer rate between the refrigerant and water.

The “slinger” Effect: The slinger sprays water droplets into the air stream flowing over the condenser coil surface. Instead of modeling the heat and mass transfer process, a simple approach was adopted here to treat the slinger effect as an air side heat transfer enhancement factor from the experimental data. Experiments were performed in the psychrometric chamber, with strictly controlled indoor condition at 80°F DB/67°F WB (26.7°C/19.4°C). The slinger effect is modeled [LBNL (1997)] as a function of the water condensate amount sprayed on the condenser coil. For this single-speed WAC, the only factor impacting the water condensate amount is the outdoor air temperature. Thus, for comparing the slinger effect, the outdoor air

temperature was varied from 90°F to 110°F (32.2°C to 43.3°C) in the outdoor chamber, which resulted in different amounts of water condensate, and hence varying sling effect. Figure 6 compares the model predicted air side heat transfer enhancement multipliers due to the sling effect to laboratory data deduced heat transfer multipliers, as a function of the ambient temperature. The laboratory data deduced heat transfer multipliers were obtained by adjusting air side heat transfer coefficient of the condenser model to match the measured performance, assuming no sling effect. Since there is a large dispersion in the laboratory measurements, deviations between the laboratory deduced and model predicted heat transfer multipliers can be up to 30%. However, the average multipliers are close; with laboratory data deduced multiplier being 1.33, and the model predicted average multiplier being 1.24. The HPDM was used to predict the incremental performance enhancement due to submerged sub-cooler and the slinger, in comparison to the baseline WAC without the submerged sub-cooler and the slinger. The results are shown in Figure 7 for R410A.

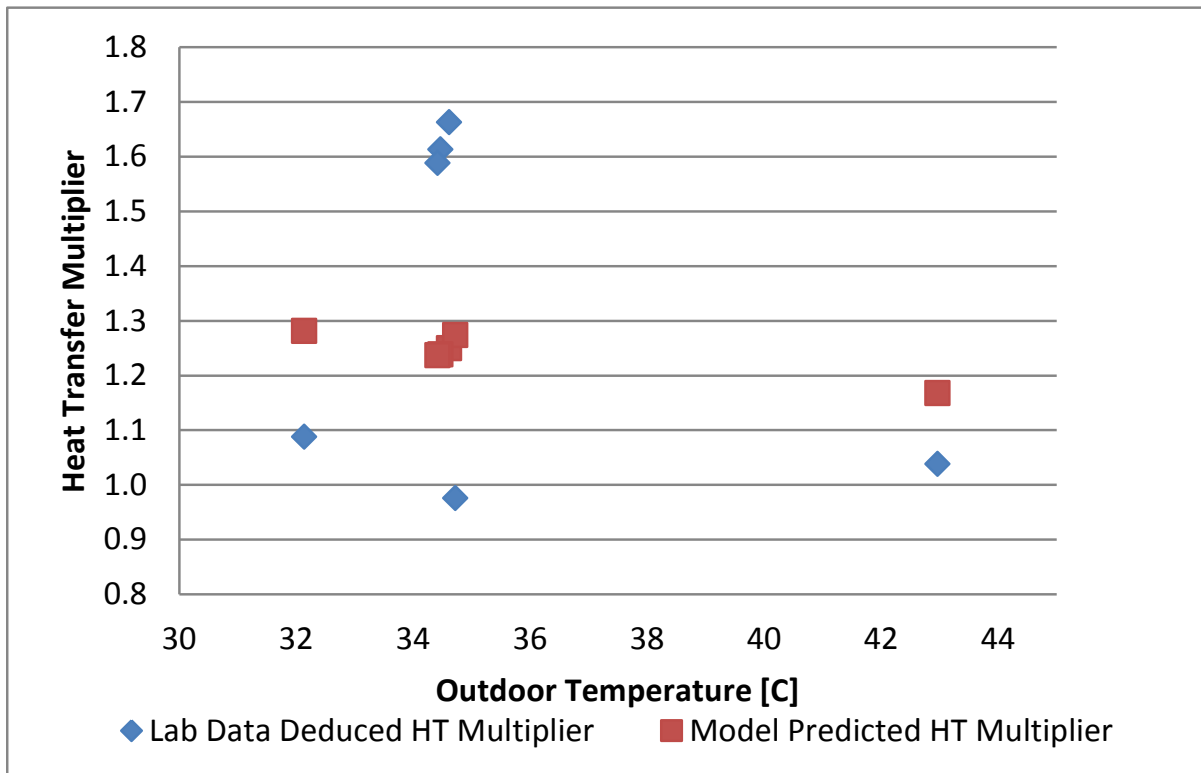


Figure 6: Heat transfer enhancement ratio due to ‘sling effect’ vs. outdoor temperature

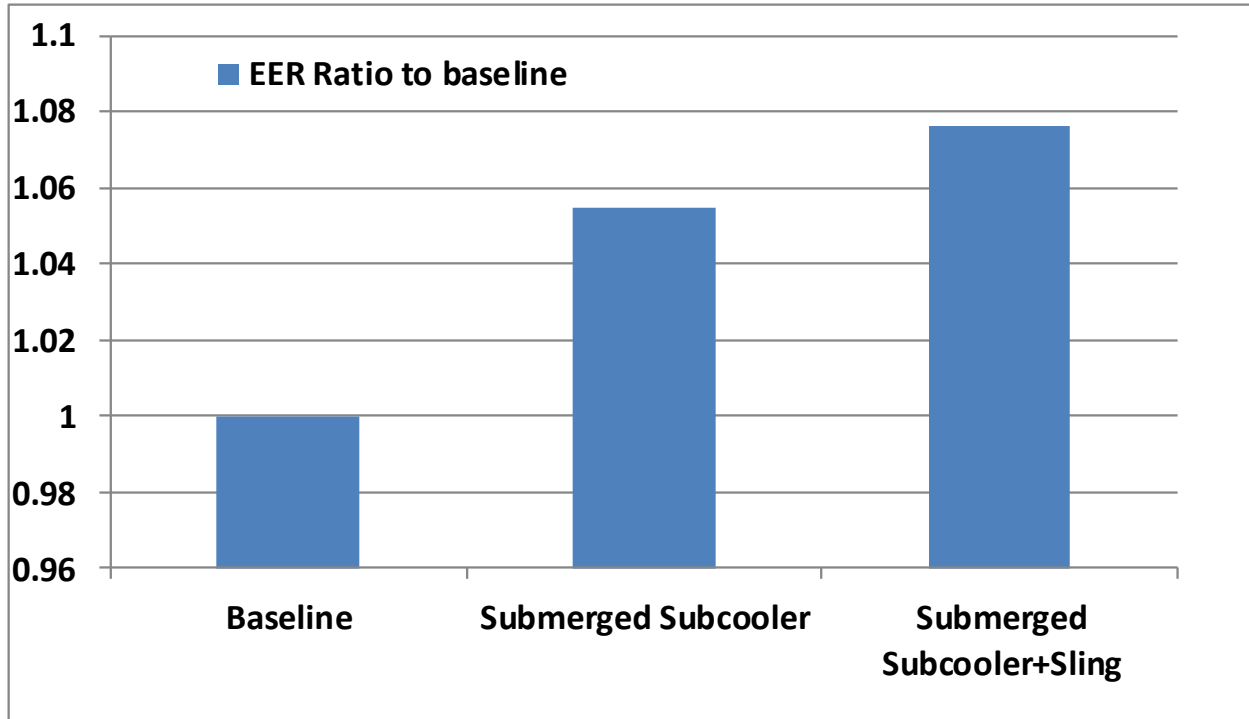


Figure 7: Modeled EER (normalized) enhancements due to submerged sub-cooler and slinger

4. COMPARISON OF ORNL MODEL WITH THE TEST DATA

After the model had been calibrated with the experimental data, the model predictions were compared with the test data over a range of ambient conditions. The measured EER is plotted against the simulated EER in Figure 8. The model predictions agree to within -0.5% to +6.5% with a standard deviation of 2.7%.

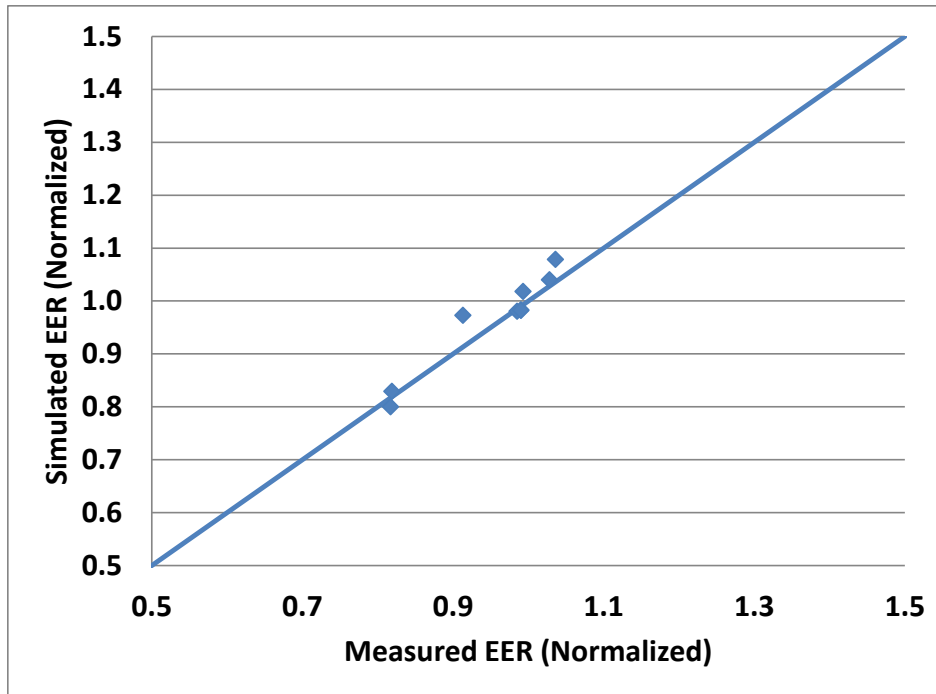


Figure 8: Variation of ‘measured EER’ with ‘simulated EER’ at different ambient temperatures for the baseline WAC with the baseline R410A refrigerant

5. OPTIMIZATION OF HEAT EXCHANGER CIRCUITRY

In order to identify the best potential replacement for R410A in WACs, simulations were performed at the standard outdoor and indoor dry bulb/wet bulb temperature conditions specified earlier. The compressor displacement volume was automatically adjusted to facilitate the same cooling capacity of 10,000 Btu/h (2.93 kW), for various refrigerants, while assuming the same isentropic efficiency of 66% and volumetric efficiency of 86% as determined for the WAC with R410A. The degrees of condenser sub-cooling and the evaporator superheat are held at 10°R (5.6K). All the simulations were run with the submerged sub-cooler and slinger.

Refrigerant side pressure loss causes a drop in the saturation temperature in a heat exchanger in the two-phase region, which effectively results in the reduction of the heat transfer driving potential in the heat exchanger. Increasing number of circuits in a heat exchanger (i.e. each circuit having fewer tubes) leads to decrease in the refrigerant side pressure loss, and hence the saturation temperature drop. However, the downside is that more circuits result in the reduction of the refrigerant flow velocity, which degrades the tube side heat transfer. Hence, there is a

trade-off between the drop in saturation temperature and the reduction in the refrigerant velocity. Therefore, the number of circuits in a heat exchanger with fixed number of tubes should be optimized to achieve the best heat transfer performance of the heat exchanger.

The relationship between the pressure loss and the drop in saturation temperature drop is unique for any refrigerant. To have a fair comparison among various refrigerants and to achieve the best efficiency of the WAC, the heat exchanger surface area and tube numbers were fixed both for the evaporator and condenser and parametric simulations were performed to optimize the number of circuits of the condenser and evaporator for each alternative refrigerant. Both the evaporator and condenser circuitries were optimized to maximize the system cooling EER while maintaining a constant cooling capacity. For example, Figures 9 and 10 illustrate contour plots of the system normalized EER at outdoor temperature 95°F (35°C) as a function of number of circuits of evaporator and condenser for R-32 and R-1234yf, respectively. Apparently, the saturation temperature of R-1234yf is more sensitive to the pressure change than R-32. The R-1234yf system requires six evaporator circuits and four condenser circuits for the optimum EER while the R-32 system requires only three evaporator circuits and two condenser circuits to achieve the best performance. Figure 11 shows the optimized evaporator and condenser circuit numbers of all the refrigerant types.

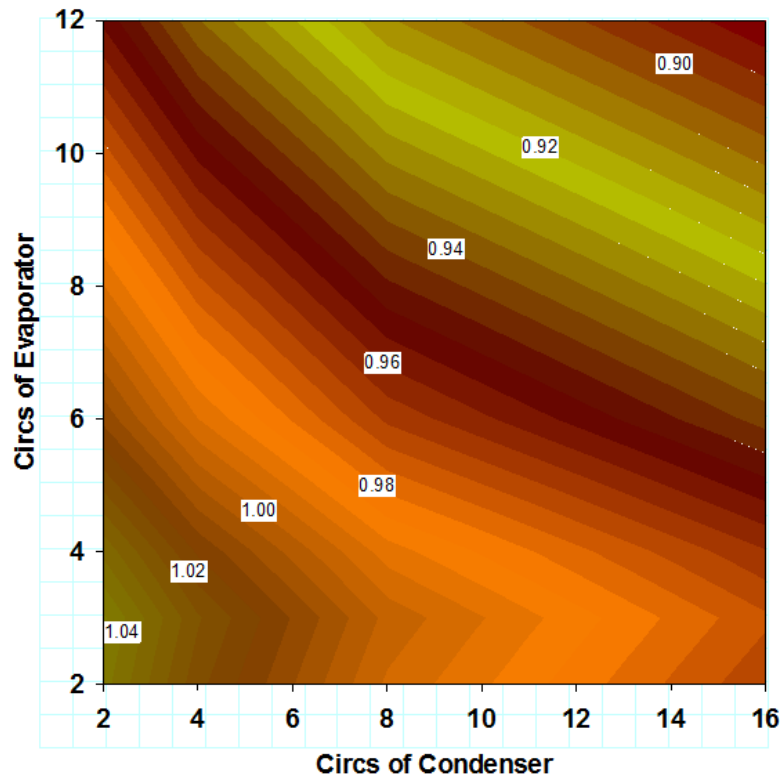


Figure 9: Number of evaporator and condenser circuits to optimize EER for R-32

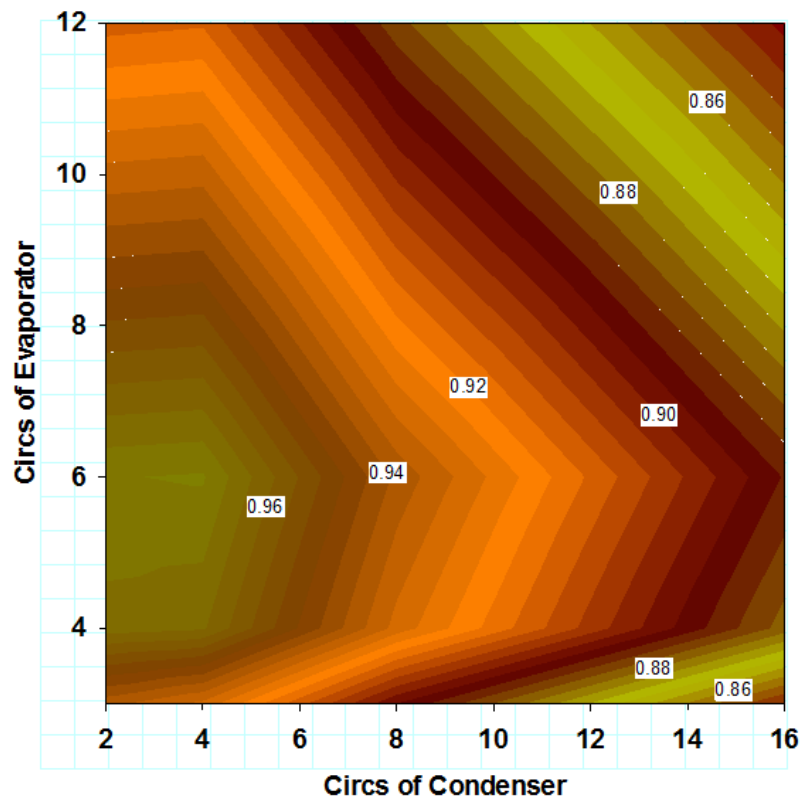


Figure 10: Number of evaporator and condenser circuits to optimize EER for R-1234yf

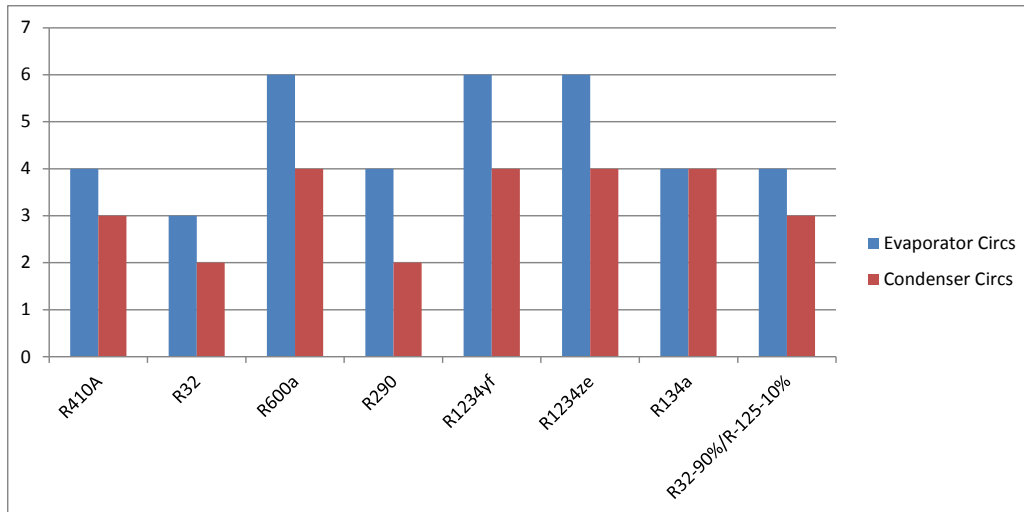


Figure 11: Optimized number of circuits in condenser and evaporator for various refrigerants

6. RESULTS AND DISCUSSION

Comparison of Required Compressor Displacement Volumes: Figure 12 illustrates the required compressor displacement volumes to achieve the cooling capacity of 10,000 Btu/h (2.93 kW) for each refrigerant, with the optimized circuit numbers. It can be seen that R410A, R32, and R32-90%/R125-10% require similar displacement volumes. It means that R32, and R32-90%/R125-10% can be suitable near “drop-in” replacements for R410A using the same compressor size. However, other refrigerants require a noticeably larger displacement volume, which implies that new compressors will need to be designed if these refrigerants were to be considered for WACs.

Comparison of Heat Exchanger Configurations: Figures 13 and 14 show the comparison of the drop in saturation temperatures in the evaporator and condenser respectively for various refrigerants, with the original and the optimized circuit numbers. In Figure 13, it can be seen that the drop in saturation temperature in the evaporator is more significant for R134a, R600a, R1234yf, and R1234ze. However, with the optimized evaporator circuitry, the corresponding drop in saturation temperature in the evaporator is reduced noticeably. Similar is the pattern for optimized circuitry in the condenser as shown in Figure 14, where the notable feature is that the optimized condenser circuitries prefer fewer circuit numbers and larger refrigerant velocity that resulted in larger drop in the saturation temperature. This occurs due to the fact that the

submerged subcooler and the water slinger enhance the condenser heat transfer, and the condenser heat transfer is less prone to the saturation temperature drop, and the large refrigerant side velocity benefits the heat transfer in both the condenser and the subcooler.

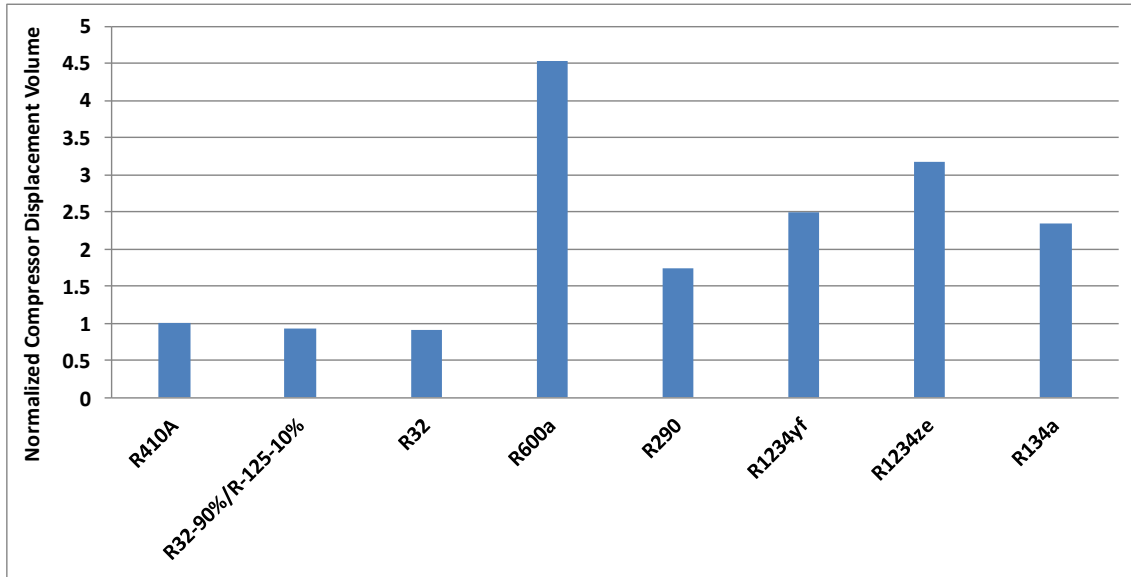


Figure 12: Normalized Compressor Displacement Volumes of Various Refrigerants

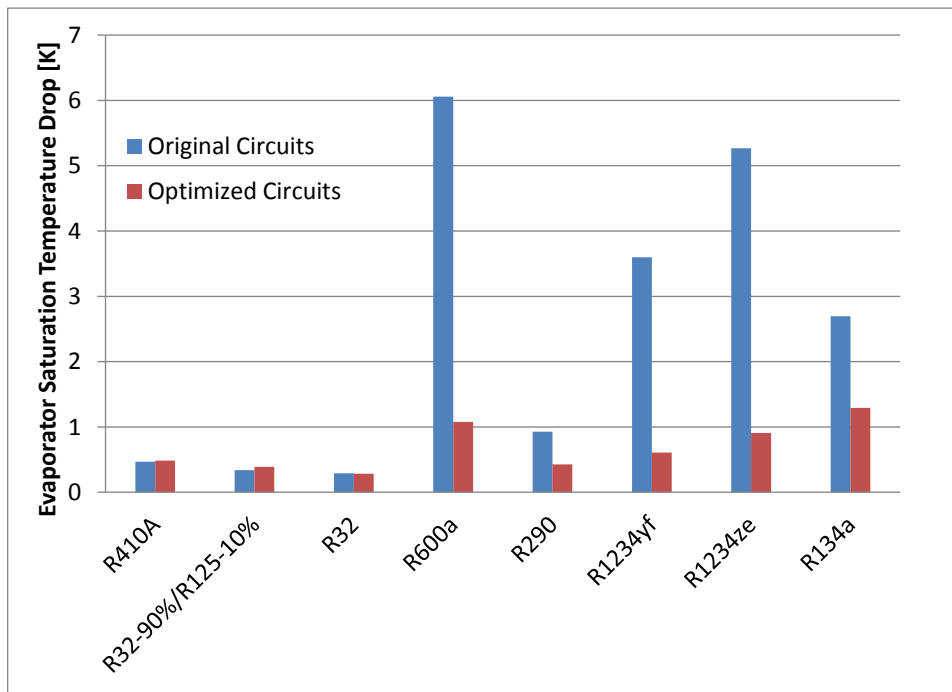


Figure 13: Comparison of the drop in evaporator saturation temperature between optimized and original circuits for various refrigerants

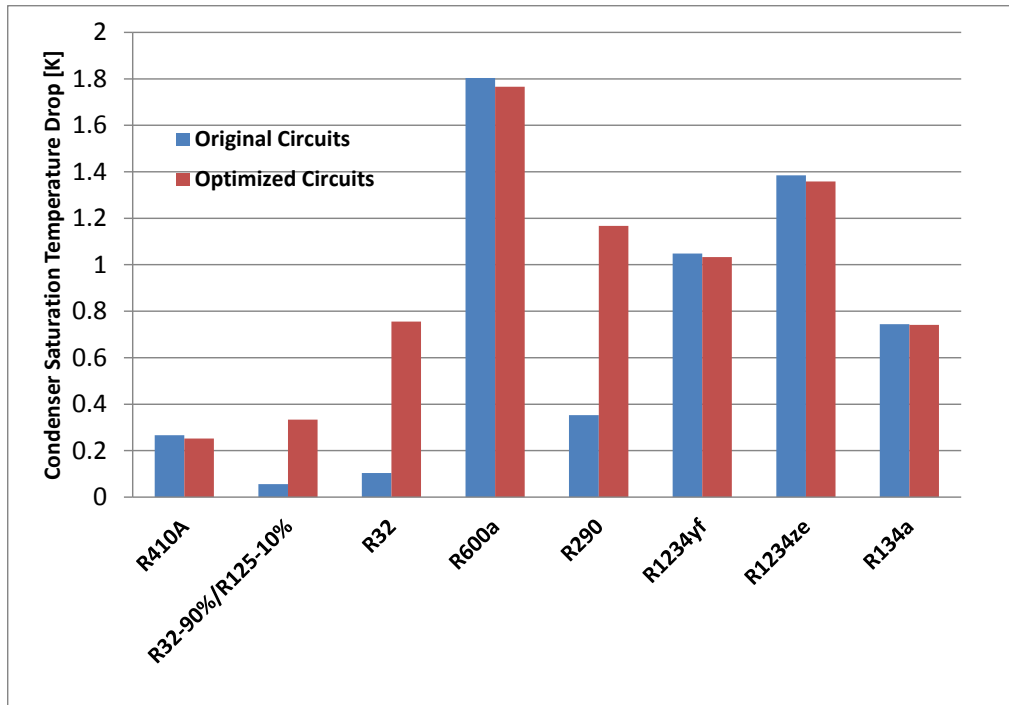


Figure 14: Comparison of the drop in condenser saturation temperature between optimized and original circuits for various refrigerants

Comparison of Compressor Discharge Temperatures: The variation of discharge temperatures of various refrigerants has been exhibited in Figure 15, where R32 shows the highest discharge temperature, which is about 30°R (16.7K) higher than R410A. It should be noted here that the “slinger” is effective in a number of ways, including reducing the condenser saturation temperature, and the discharge temperature by about 7°R (3.9K) in comparison to that without the slinger.

Comparison of Energy Efficiency Ratio (EER): Figure 16 illustrates the normalized EERs of alternative refrigerants at the outdoor temperature of 95°F (35°C) - normalized to the EER of the R410A unit with the original WAC circuitry using R410A). It can be seen that R32 results in the highest EER with the same heat exchangers’ surface area as that of the base unit. This is followed by the mixture of R32/R125 (90%/10%), R290, while all other refrigerants perform worse than R410A.

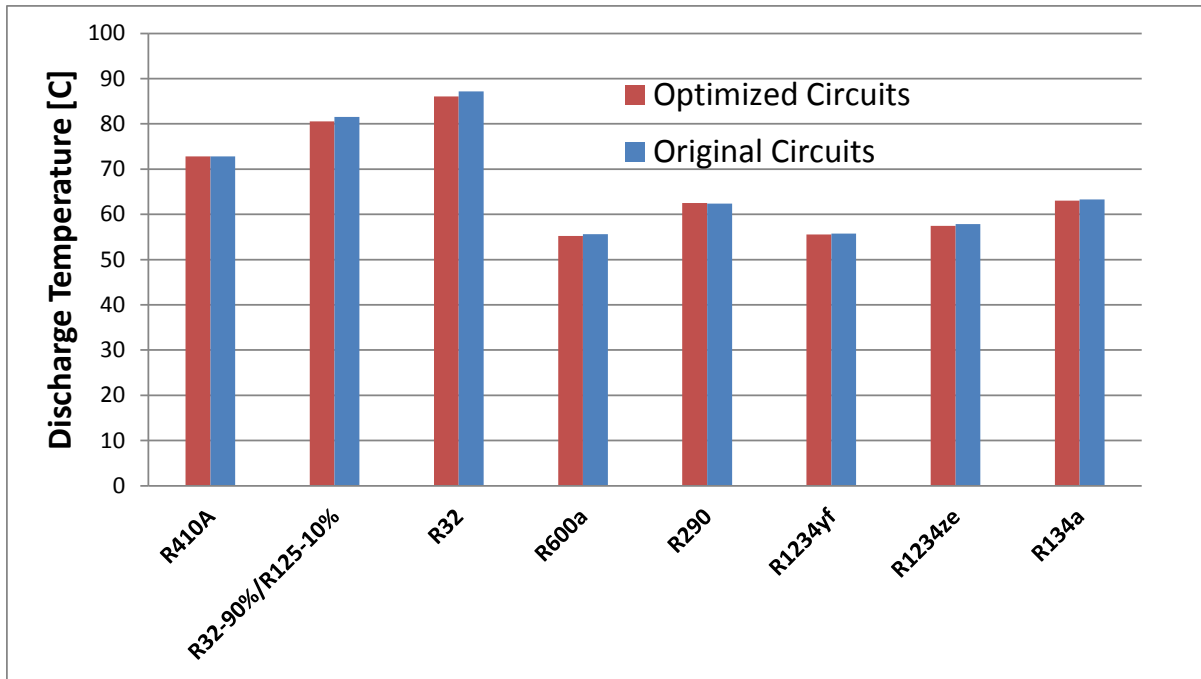


Figure 15: Compressor Discharge Temperatures of Various Refrigerants

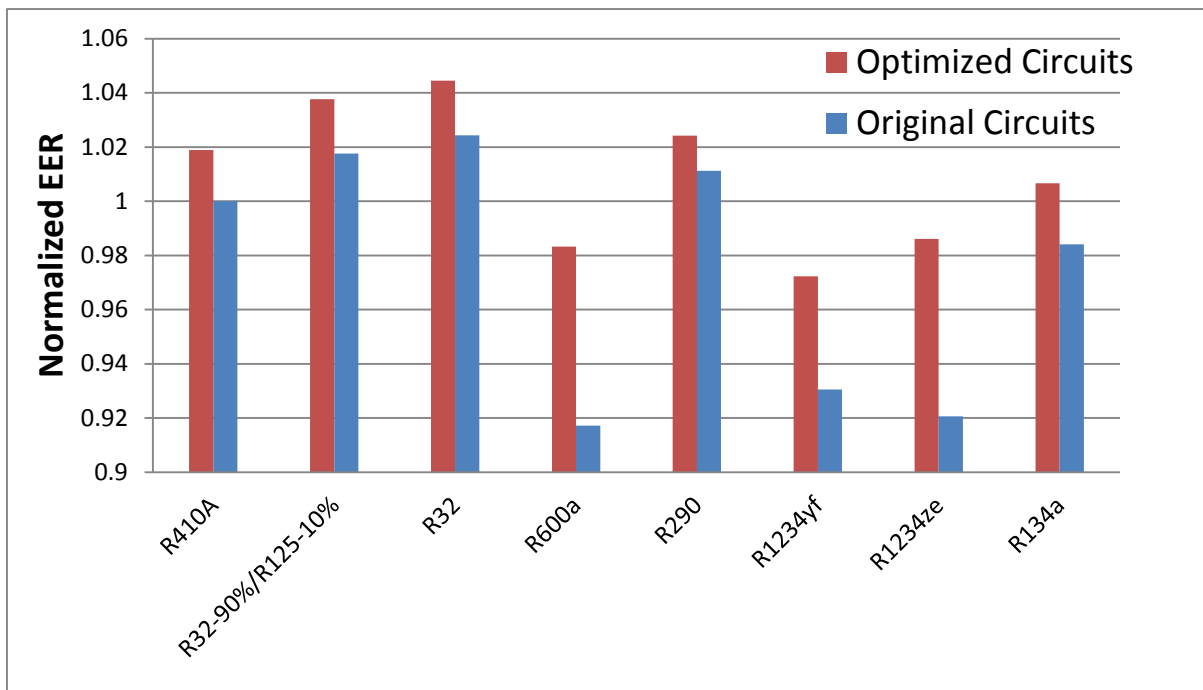


Figure 16: Normalized EERs of Various Refrigerants at 95°F (35 °C) ambient temperature – Normalized EER for R410A = 1.00

7. CONCLUSIONS

A high efficiency window air conditioner, using R-410A, was extensively tested and modelled in this investigation. The experimental data demonstrated that the combination of a submerged subcooling loop and the ‘slinger’ effect boosted the system EER at 95°F (35°C) by almost 8% (Figure 7). The calibrated window air conditioner system model was used to evaluate the lower GWP alternative refrigerants (for R410A) as R32, R600a, R290, R1234yf, R1234ze, and a mixture of R32/R125 with molar concentrations of 90%/10%. From the perspective of efficiency possibility to be a ‘drop in’ replacement for R410A, R32 is clearly the best choice since it results in the highest EER without making any modification in components of the tested WAC. However, R32 suffers from slight flammability concerns and it also has the highest discharge temperature of up to 200°F (93.3°C) at 95°F (35°C) ambient. An alternative option is the mixture of R32/R125 with the respective molar concentration of 90%/10% for balancing between efficiency and flammability. R1234yf and R1234ze, i.e. two HFO refrigerants, demonstrated the worst EERs in the simulations, and require larger compressor displacement volumes to achieve the same cooling capacity. Clearly, both the compressor and the heat exchangers must be re-optimized for these HFO refrigerants. Between the two natural refrigerants, R290 can be a potential replacement for R410A, since it leads to a higher EER with the same heat exchanger configurations. However, R290 needs a larger compressor displacement volume than R410A and has significant flammability issues. R32 has about a 67.5% lower GWP than R410A and also enhances the system EER by about 4% and hence offers the best combination of advantages - less operating cost, less electrical demand, and an increase in the overall environmental friendliness.

ACKNOWLEDGMENTS

The authors also acknowledge the support of Building Technologies Office of the US Department of Energy under contract DE-AC05-00OR22725 with UT-Battelle for their financial support and industry partner for their in-kind and technical support. Special thanks are due to colleagues Messrs. Van Baxter, Edward Vineyard and Keith Rice for their continuous support during the project.

REFERENCES

- ANSI/AHRI Standard 540, 2007, “Positive Displacement Refrigerant Compressors and Compressor Units”, Air-Conditioning and Refrigeration Institute, Arlington, VA
- Braun. J.E., Klein. S.A, and Mitchell, J.W., 1989, “Effectiveness models for cooling towers and cooling coils”, ASHRAE Transactions, 95(2), pp. 164-174.
- DOE, 2011, “Residential Clothes Dryers and Room Air Conditioners Direct Final Rule Technical Support Document”, 4/18/2011; updated on 03/02/2012, http://www1.eere.energy.gov/buildings/appliance_standards/residential/residential_clothes_dryers_room_ac_direct_final_rule_tsd.html
- e-CFR Title 10: “Energy, Part 430- Energy conservation program for consumer products”, 2014, <http://www.ecfr.gov/cgi-bin/text-idx?SID=19211021fb068617aba13063da4e959a&node=10:3.0.1.4.18.3.9.2&rgn=div8>
- EIA (2009); Residential Energy Consumption Survey, US DOE Energy Information Administration, <http://www.eia.gov/consumption/residential/data/2009/>
- Lawrence Livermore National Laboratory (LBNL), 1997, “Technical support document for energy conservation standards for room air conditioners: Volume 2 - Detailed analysis of efficiency levels”, Docket Numbers EE-RM-90-201 & EE-RM-93-801-RAC, September.
- Nogueira, L A H, 2013, “Package of measures to promote efficient air conditioning”, ADEME, World Energy Council Study, http://www.wec-policies.enerdata.eu/Documents/cases-studies/Measures_to_promote_efficient_air_conditioning.pdf
- Lemmon, E.W., Huber, M.L., McLinden, M.O. NIST Standard Reference Database 23: Reference Fluid Thermodynamic and Transport Properties-REFPROP, Version 9.1, National Institute of Standards and Technology, Standard Reference Data Program, Gaithersburg, 2013; http://www.boulder.nist.gov/div838/theory/refprop/Frequently_asked_questions.htm#REFPROPReference
- Rice, C. K., Jackson, W. L. , Fischer, S. K. and Ellison, R. D. , 1981, Design optimization and the limits of steady-state heating efficiency for conventional single speed air-source heat pumps, Contract No. W-7405-eng-26, ORNL/CON-63, Department of Energy.
- Shen, B. and P. K. Bansal, 2014, Assessment of environmentally friendly refrigerants for window air conditioners, ID2275, Proc. 15th International Refrigeration and Air Conditioning Conference, Purdue University, West Lafayette, July 14-17.
- Shen, B. and C. K. Rice, 2014, HVAC System Optimization with a Component Based System Model – New Version of ORNL Heat Pump Design Model, Purdue HVAC/R Optimization short course, International Compressor & refrigeration conferences at Purdue, Lafayette, USA, 2014
- Thome J.R. and Jean Ei Hajal, 2002, "On recent advances in modelling of two-phase flow and heat transfer", 1st Int. Con. on Heat Transfer, Fluid mechanics, and Thermodynamics, Kruger Park, south Africa TJ1, 8-10 April.
- Thome J. R., J. El Hajal, and A. Cavallini, 2003a, “Condensation in horizontal tubes, part 1: two-phase flow pattern map”, International Journal of Heat and Mass Transfer, 46(18), Pages 3349-3363.

- Thome J. R., J. El Hajal and A. Cavallini, 2003b, “Condensation in horizontal tubes, part 2: new heat transfer model based on flow regimes”, *International Journal of Heat and Mass Transfer*, 46(18), Pages 3365-3387.
- Winkler, J., C. Booten, D. Christensen and J. Tomerlin, 2013, “Laboratory performance testing of residential window air conditioners”, NREL/TP-5500, 57617, July.